Biosensors and Bioelectronics 90 (2017) 224–229

Contents lists available at ScienceDirect

Biosensors and Bioelectronics

journal homepage: www.elsevier.com/locate/bios

Excellent storage stability and sensitive detection of neurotoxin quinolinic acid

Ranjana Singh[a], Sunayana Kashyap[b], Suveen Kumar[c], Shiju Abraham[a], Tejendra K. Gupta[a], Arvind M. Kayastha[d], Bansi D. Malhotra[c], Preeti Suman Saxena[b,*], Anchal Srivastava[a,*], Ranjan K. Singh[a,*]

[a] Department of Physics, Institute of Science, Banaras Hindu University, Varanasi 221005, India
[b] Department of Zoology, Institute of Science, Banaras Hindu University, Varanasi 221005, India
[c] Department of Biotechnology, Delhi Technological University, Main Bawana Road, Delhi 110042, India
[d] School of Biotechnology, Institute of Science, Banaras Hindu University, Varanasi 221005, India

ARTICLE INFO

Keywords:
Quinolinic Acid
QPRT
Enzyme
Neurotoxin
Bio-electrodes

ABSTRACT

Quinolinic acid (QA) is a metabolite of tryptophan degradation obtained through kynurenine pathway, produced naturally in the mammalian brain as well as in the human cerebrospinal fluid. The presence of QA ~10–40 μM is a clear indicator of many neurological disorders as well as deficiency of vitamin B_6 in human being. In the present work; rapid, sensitive and cost-effective bio-electrodes were prepared to detect the trace amount of endogenous neurotoxin (QA). Cyclic voltammetry (CV) and differential pulse voltammetry (DPV) studies were carried out to measure the electrochemical response of the fabricated bio-electrodes as a function of QA concentrations. These devices were found to exhibit desirable sensitivity of ~7.86 mA μM^{-1} cm^{-2} in wide concentration range (6.5 μM-65 mM). The lower detection limit of this device is as low as 6.5 μM and it has excellent storage stability of ~30 days. The capability of the proposed electrochemical bio-sensor was also checked to detect QA in the real samples (human serum). These results reveal that the use of this electrochemical bio-sensor may provide a potential platform for the detection of QA in the real samples for the prior detection of many diseases.

1. Introduction

Quinolinic acid (pyridine 2,3-dicarboxilic acid, hereafter referred as QA) (Heyes et al., 1992) occurs naturally in the mammalian brain in nano-molar as well as in the human cerebrospinal fluid in several nano-molar to micro-molar amounts (Heyes et al., 1992; Chen et al., 2009; Schwarcz and Pellicciari, 2002). The presence of QA is found below 100 nM, whereas the increased level of this molecule (10–40 μM) can be detected in pathological conditions (Guillemin, 2012; Leipnitz et al., 2005). The increased level of this molecule is known to be responsible for many neurological disorders such as Alzheimer, (Guillemin and Brew, 2002) Huntington disease (Schwarcz et al., 2010) and HIV associated dementia (HAD) (Guillemin et al., 2004). The presence of QA also affects the function of neurons by the activation of *N*-methyl-D-aspartate (NMDA) receptors (Birley et al., 1982; Stone and Connick, 1985). Apart from these effects, its elevated level (30–164 μM) has also been recognized as a clear indicator of deficiency of vitamin B_6 in the human being (Brown et al., 1965). All these reports reveal that the elevated level of QA can be used to detect the presence of many diseases (Guillemin, 2012; Leipnitz et al., 2005; Guillemin and Brew, 2002; Schwarcz et al., 2010; Guillemin et al., 2004; Birley et al., 1982; Stone and Connick, 1985; Brown et al., 1965). Hence there is urgent need to fabricate; rapid, cost-effective, durable and sensitive sensor that can be used to detect the trace amount of QA for the early detection of many diseases as mentioned above (Guillemin, 2012; Leipnitz et al., 2005; Guillemin and Brew, 2002; Schwarcz et al., 2010; Guillemin et al., 2004; Birley et al., 1982; Stone and Connick, 1985; Brown et al., 1965).

Several detection techniques such as gas chromatography, mass spectrometry (During et al., 1989; Shoemaker and Elliott, 1991) liquid-chromatography (Patterson and Brown, 1980), thin layer chromatography (Taguchi et al., 1983), radio enzymatic assay (Foster et al., 1986) and capillary electrophoresis-mass spectrometry (Wang et al., 2013) can be utilized to determine the trace amount of QA in the biological samples. All these reported methods are time consuming as well as suffer from lack of selectivity, sensitivity and stability. Liquid

* Corresponding authors.
E-mail addresses: pssaxena@rediffmail.com (P.S. Saxena), anchalbhu@gmail.com (A. Srivastava), ranjanksingh65@rediffmail.com (R.K. Singh).

http://dx.doi.org/10.1016/j.bios.2016.11.053
Received 26 October 2016; Accepted 22 November 2016
Available online 23 November 2016
0956-5663/ © 2016 Published by Elsevier B.V.

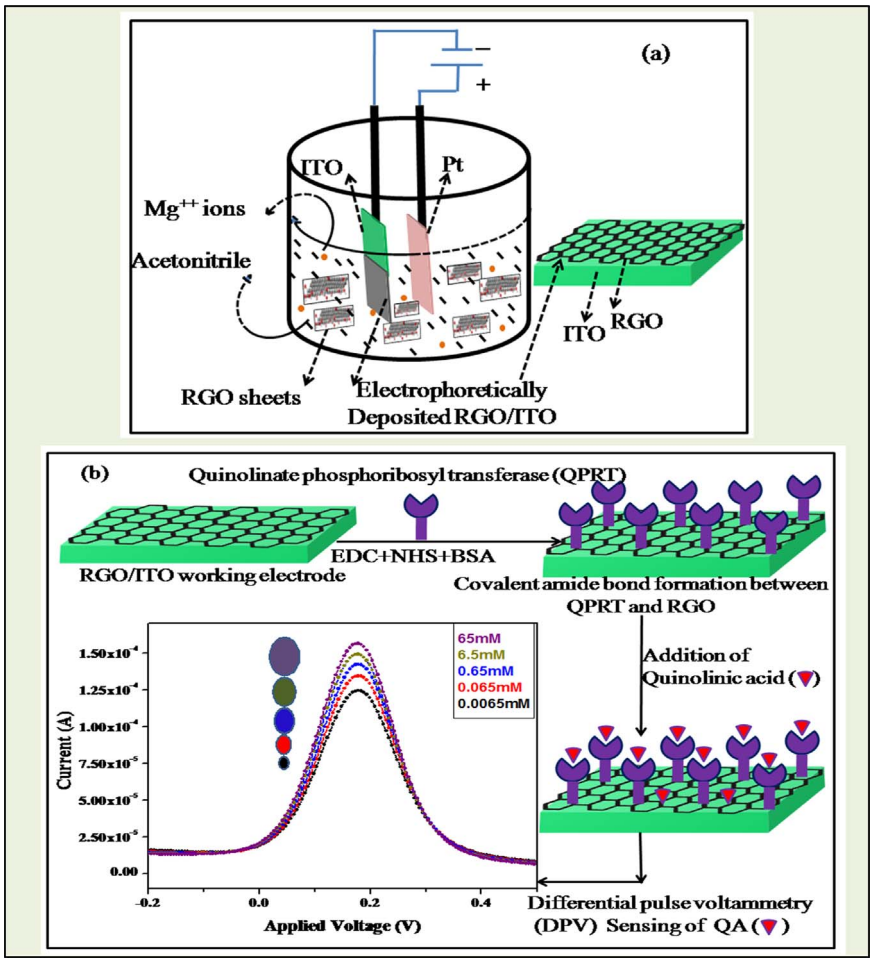

Fig. 1. Schematics for the (a) Fabrication of working electrode RGO/ITO by using electrophoretic deposition (EPD) technique and (b) immobilization of quinolinate phosphoribosyl transferase (QPRT) on working electrode RGO/ITO treated with EDC/NHS and BSA and sensing of QA via differential pulse voltammetry (DPV) technique.

chromatography with fluorimetric detection (Mawatari et al., 1995) has been reported to determine the trace amount of QA. However, this method suffers from certain limitations such as tedious procedure to handle the sample, to protect it from light and lack of selectivity. Fluorimetric detection of QA, based on catalytic activity of horseradish perioxidase (HRP) (Odo et al., 2009) in presence of hydrogen peroxide (H_2O_2) has been available to determine trace amount of QA. In this method; QA acquires fluorescing property but some reducing and oxidizing substances were found to affect the fluorescent derivatization of QA with HRP in presence of H_2O_2. Although sensitivity associated with this method is high but lack of selectivity, stability and time consuming procedure has remained as a challenge. Hence to remove all these short-comings, fabrication of such a sensing device having excellent storage stability and quick response is highly desirable for the early detection of the trace amount of QA.

Electrochemical bio-sensors have become more powerful sensing devices in recent years (Chikkaveeraiah et al., 2009) because of its quick response, sensitivity, simplicity, reproducibility and selectivity. These sensing devices require low reagents consumption, ease of fabrication, miniaturization and continuous monitoring of the analytes (Srivastava et al., 2011). As synthesized reduced graphene oxide (RGO, derivative of graphene) has become a promising material for biosensing applications recently in comparison to the graphene oxide (GO), (Srivastava et al., 2011; Schwierz, 2010; Park et al., 2012; Han et al., 2007; Pumera et al., 2010; Pumera, 2011; Huang et al., 2010, 2011; Srivastava et al., 2013). Chemically active RGO has large surface area, sufficient functional groups, potential to facilitate electron transfer from enzymes and proteins, cost-effective and easy to handle which are the essential properties of the electrochemical bio-sensors (Pumera et al., 2010; Pumera, 2011; Compton et al., 2011).

We have fabricated the cost-effective bio-sensor to detect the trace amount of QA. Various parameters (reproducibility, selectivity, magnitude of currents, linear coefficient and standard deviation) have been calculated for these devices. These bio-electrodes have good sensitivity of 7.86 mA μM^{-1} cm^{-2} with a wide range (6.5 μM– 65 mM) responses. It has good selectivity and excellent storage stability of ~30 days. The observed properties of the present bio-sensor are exciting and it can be useful to develop electrochemical bio-sensor for the early detection of QA. In the present work, we report results of the studies relating to the development of an electrochemical bio-sensing technique differential pulse voltammetry (DPV) to detect the trace amount of endogenous neurotoxin QA in the real samples (serum) also.

2. Experimental section

2.1. Materials

Quinolinate phosphoribosyl transferase (QPRT) enzyme was procured from KrishgenBiosystems, New Delhi India. Quinolinic acid (QA), 2, 6 pyridine di-carboxylic acid (PD), graphite flakes, acetonitrile, magnesium nitrate, sodium citrate, *N*-hydrooxysuccinimide (NHS), *N*-ethyl-*N*-(3-dimethylaminopropyl) carbodiimide (EDC), bovine serum albumin (BSA) and other analytical grade chemicals used in this work were procured from Sigma-Aldrich, India. All these materials were used without further purification.

2.2. Synthesis of reduced graphene oxide (RGO)

Graphene oxide (GO) was prepared by chemical route using Hummer's method (Marcano et al., 2010) and reduced graphene oxide (RGO) was obtained by reduction of GO with sodium citrate (Zhang et al., 2011). In this method, 100 mg sodium citrate was added into 10 ml aqueous suspension of GO (1 mg/ml) and the solution was stirred magnetically at 60 °C for ~6 h. Change in color from brown to black clearly indicates the reduction of GO to RGO. The RGO was treated in the following sequence; cooled down to room temperature, centrifuged at 10,000 rpm, washed with triple distilled water repeatedly and finally dried in the oven. The dried RGO powder was dispersed into water and acetonitrile for further use.

2.3. Preparation of RGO/ITO electrodes

Electrophoretic deposition (EPD) (Srivastava et al., 2013, 2012) technique was employed to fabricate RGO films on indium tin oxide (ITO) coated glass plate with sheet resistance ~30 Ω cm^{-1}. In this method, ITO-coated glass substrate acted as cathode and a platinum (Pt) foil (1 cm×2 cm) acted as an anode. These electrodes were kept parallel separated by 1 cm in a colloidal suspension of RGO prepared in acetonitrile (0.5 mg dl^{-1}). The 10^{-4}-10^{-5} M solution of Mg $(NO_3)_2 \cdot 6H_2O$ was added to the RGO suspension to enhance the deposition rate of RGO sheets on the cathode (ITO) (Wang et al., 2009; Compton et al., 2011). During the EPD process, DC voltage (150 V) was applied for two minutes. All these process involved in the preparation of working electrode has been depicted schematically in Fig. 1(a).

2.4. Immobilization of QPRT enzyme onto the RGO/ITO electrodes surface

An enzyme QPRT was covalently attached to RGO/ITO electrode. Prior to covalent attachment of the enzyme, COOH group of RGO was activated using EDC as a coupling agent and NHS as an activator. The COOH groups of RGO activated by following EDC/NHS chemistry (Srivastava et al., 2013; Sarkar and Nicholson, 1996) bind to the NH_2 groups of QPRT which results into the covalent amide bond (CONH) formation between RGO and QPRT. During the process of covalent attachment of QPRT to RGO/ITO electrode, 10 µl of QPRT enzyme (concentration 300 µg/ml) was freshly prepared in Tris HCl buffer (PH 8.0) and it was uniformly spread on the EDC/NHS activated RGO/ITO electrode [see Fig. 1(b)]. This electrode; immobilized with QPRT was incubated in humid chamber at room temperature for ~6 h. Since QPRT consisted of amino acids residues having NH_2 groups hence the formation of covalent immobilization was proposed via interaction between NH_2 functional groups of QPRT and COOH groups of RGO. Non-specific sites of the bio-electrodes were blocked by using bovine serum albumin (BSA). The amide bond formation was experimentally verified by FTIR spectra of QPRT/RGO. Schematic of immobilization of QPRT on working electrode RGO/ITO treated with EDC/NHS and BSA along with sensing of QA via differential pulse voltammetry (DPV) technique has been shown in Fig. 1(b).

3. Characterization

Structural and morphological characterizations were carried out using scanning electron microscopy (SEM, Philips XL 20), transmission electron microscopy (TEM-FEI Tecnai G2 electron microscope) and X-ray diffraction (XRD, Rigakuminiflex II). Raman (In-via Raman spectrometer, Renishaw), FTIR (Spectrum 65 FT-IR spectrometer, Perkin Elmer), UV–Visible (Lambda 25 UV–Visible spectrometer, Perkin Elmer) spectroscopic techniques were employed to characterize the as synthesized RGO. All the electrochemical measurements such as cyclic voltammetry (CV) and differential pulse voltammetry (DPV) were carried on Auto lab Potentiostat/Galvanostat (Eco Chemie, Netherlands) using three electrode cell configurations. Bio-electrode (QPRT/BSA/RGO/ITO), platinum foil and Ag/AgCl electrodes were used as working, counter and reference electrodes, respectively. The mixture of 5 mM $Fe(CN)_6^{4-}$ (Ferrocynide) and 5 mM $Fe(CN)_6^{3-}$ (Ferricynide) was used as the redox probe.

4. Results and discussion

4.1. Microstructural studies of RGO

SEM images of RGO shown in Fig. S1(a) indicates the uniform and sheet like morphology which is extended to several micrometers. Further, it is clearly visible that the thin layered RGO sheets consist of several wrinkles and folds. These wrinkles and folds might have developed due to defects and functional groups present in the carbon lattice. Fig. S1(b) shows TEM micrograph of RGO, which reveals a few layers of RGO sheets along with wrinkles and folds. HRTEM images in the inset of Fig. S1(b) indicates that the average inter-planar spacing of the lattice fringes of RGO is found to be ~3.5 Å.

The Raman spectrum of RGO has been shown in Fig. S1(c) containing four Raman bands observed at 1352, 1595, 2708 and 2930 cm^{-1}. The most prominent Raman band observed at 1352 cm^{-1} is assigned as D band which is attributed to the disorder present in the RGO. This structural disorder may be correlated to the oxygen functional groups as well as point defects present in the system. The Raman band centered at 1595 cm^{-1} is a well-defined; G band which represents the presence of sp^2 bonded carbon atoms. Overtone of D band i.e. 2D band is found at 2708 cm^{-1}. The presence of this overtone is clearly related to the dispersive nature as a function of frequency (Srivastava et al., 2012).

The X-ray diffraction (XRD) pattern of RGO which has been used as a working electrode for electrochemical bio-sensing studies recorded in the range of 10–75° is shown in Fig. S1(d). In the XRD pattern of RGO, an intense and broad peak with a 2θ value at around 25.28° is observed and assigned to the (00.2) (Srivastava et al., 2013) reflection plane corresponding to an inter-planner spacing of 0.352 nm, which is in good agreement with the HRTEM study [discussed in inset of Fig. S1(b)]. In addition to this, another peak of lower intensity is found at ~43.3° which is assigned to the (00.1) reflection plane of RGO (Srivastava et al., 2013). UV–Visible absorption spectrum of chemically synthesized RGO is shown in Fig. S1(e) where triple distilled water was taken as reference to record UV–Vis spectrum of RGO. The absorption peak at 268 nm can be assigned as π-π* transition of aromatic C=C bonds (Srivastava et al., 2013). Figs. S1(a), S1(b), S1(c), S1(d) and S1(e) have been provided in the Supplementary material.

4.2. FTIR spectroscopic studies of RGO, QPRT and QPRT/RGO electrodes

The IR spectra of RGO, QPRT and QPRT/RGO have been shown by (A), (B) and (C), respectively in Fig. 2(a). The IR bands observed at 1650 and 1400 cm^{-1} are attributed to stretching and bending mode vibrations of C=O and O-H bonds of carboxyl groups present in the RGO respectively. The COH and C=C stretching mode of vibrations are obtained at 1110 cm^{-1}, 1631 cm^{-1}, respectively. A broad band observed at 3453 cm^{-1} is assigned to stretching vibration of OH group. It is important to note that the IR spectra were taken in aqueous medium. The OH bonds of water strongly absorb at ~3453 cm^{-1} which overlaps with OH absorption of RGO. The OH stretching band of RGO is sharp. The OH stretching band of water being broad and strong hides the OH stretching band of RGO. New IR band of QPRT/RGO is obtained 985 cm^{-1} due to OH bending vibration of carboxylic group. While stretching vibrational mode corresponding to CN becomes prominent and is observed at 1215 cm^{-1}. The intensity of stretching mode of C=O in QPRT/RGO is found to be enhanced and blue shifted which confirms the amide bond formation between carboxylic and amino group of RGO

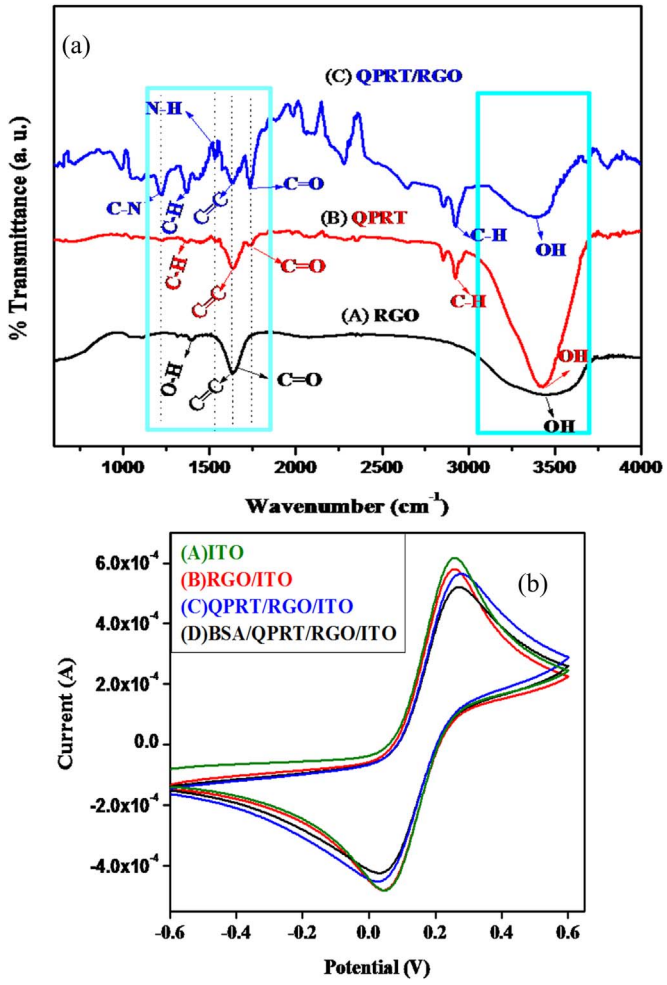

Fig. 2. (a) FT-IR spectrum of (A) RGO (B) QPRT and (C) QPRT/ RGO 3(b) CV curves of (A) ITO (B) RGO/ITO (C) QPRT/RGO/ITO and (D) BSA/QPRT/RGO/ITO electrodes.

and QPRT, respectively.

4.3. Electrochemical studies

The cyclic voltammetry (CV) studies of the fabricated electrodes were conducted in phosphate buffer solution (PBS) of pH 7.0 containing 0.9% NaCl and 5 mM solution of $[Fe(CN)_6]^{3-/4-}$. Fig. 3(b) shows cyclic voltammetry (CV) studies of ITO, RGO/ITO, QPRT/RGO/ITO and BSA/QPRT/RGO/ITO electrodes. It was found from the [Fig. 2(b)]

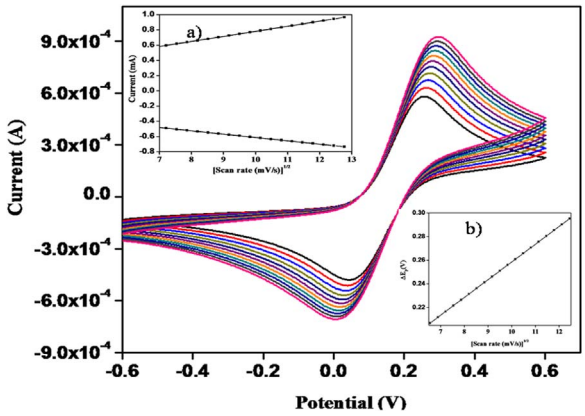

Fig. 3. Scan rate studies of RGO/ITO [Inset (a) magnitude of oxidation and reduction current generated as response of square root of scan rate (mV/s), Inset (b) potential as function of square root of scan rate] electrodes.

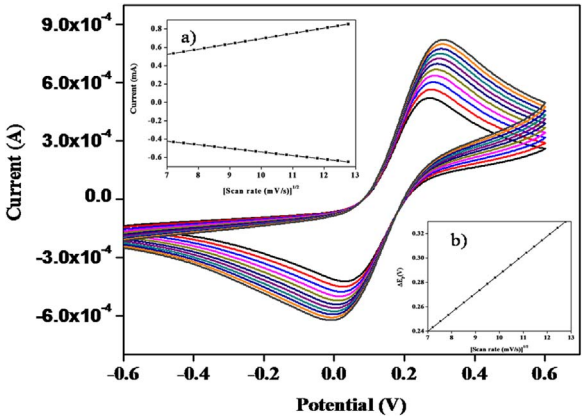

Fig. 4. Scan rate studies of BSA/QPRT/RGO/ITO [Inset (a) magnitude of oxidation and reduction current generated as response of square root of scan rate (mV/s), Inset (b) potential as function of square root of scan rate] electrodes.

that the magnitude of current for RGO/ITO electrode (Peak current 0.580 mA) is lower than that of bare ITO electrode (Peak current 0.616 mA), which indicated the reduction in electron transfer between solution and RGO/ITO interface. The immobilization of QPRT onto the RGO/ITO electrode further lowers the magnitude of peak current (0.565 mA) as compared to that of the RGO/ITO electrode. Bovine serum albumin (BSA) has been used for blocking of non-specific sites of QPRT/RGO/ITO bio-electrode. It was observed that magnitude of the peak current decreased again to 0.521 mA after coating of BSA on the surface of QPRT/RGO/ITO electrode. This reduction in peak current can be assigned due to adsorption of BSA on RGO/ITO sites of the QPRT/RGO/ITO immunoelectrode. To investigate the interfacial kinetics of the fabricated electrodes and bio-electrodes (RGO/ITO and BSA/QPRT/RGO/ITO) scan rate studies were conducted through CV. Fig. 3 and Fig. 4 show the observed CV response of RGO/ITO and BSA/QPRT/RGO/ITO electrodes respectively as a function of the scan rate (50–150 mV/s). A shift was observed in the redox peaks with increase in scan rate. It was also observed that cathodic (Ipc) and anodic peak (Ipa) currents both vary linearly with square root of the scan rate [insets (a) in Fig. 3 and Fig. 4], which indicated that the electrochemical reaction was a diffusion-controlled process (Kumar et al., 2015). The slopes and intercepts for the bio-electrodes RGO/ITO, and BSA/QPRT/RGO/ITO can be given by Eqs. (1–4):

$$I_{pc(RGO/ITO)} = [0.066\ mA(s/mV) \times (\text{scan rate}(mV/s))^{1/2}] + 0.119\ mA,\quad R^2 = 0.999,\ SD = 7.26 \times 10^{-3} \tag{1}$$

$$I_{pa(RGO/ITO)} = -[0.044\ mA(s/mV) \times (\text{scanrate}(mV/s))^{1/2}] - 0.175\ mA,\quad R^2 = 0.999,\ SD = 5.51 \times 10^{-3} \tag{2}$$

$$I_{pc(BSA/QPRT/RGO/ITO)} = [0.058\ mA(s/mV) \times (\text{scanrate}(mV/s))^{1/2}] + 0.120\ mA,\quad R^2 = 0.999,\ SD = 5.13 \times 10^{-3} \tag{3}$$

$$I_{pa(BSA/QPRT/RGO/ITO)} = -[0.039\ mA(s/mV) \times (\text{scan rate}(mV/s))^{1/2}] - 0.152\ mA,\quad R^2 = 0.999,\ SD = 4.45 \times 10^{-3} \tag{4}$$

The difference of cathodic (E_{pc}) and anodic (E_{pa}) peak potentials ($\Delta E_p = E_{pc} - E_{pa}$) and square root of scan rate for RGO/ITO and BSA/QPRT/RGO/ITO electrodes exhibit a linear relationship and follow Eqs. (5) and (6). A good linear relationship indicates the facile electron transfer from medium to the electrodes [inset (b) in Figs. 3 and 4].

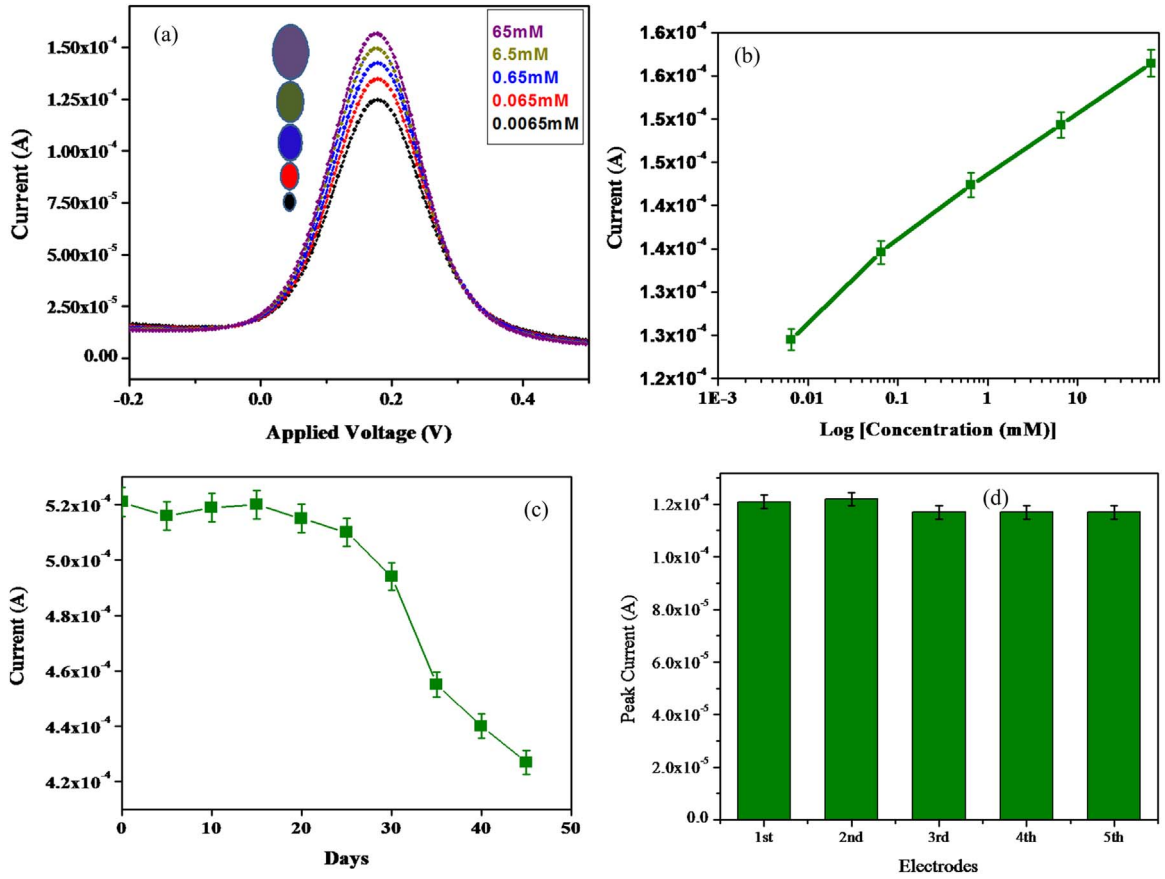

Fig. 5. (a) Electrochemical current response studies (differential pulse voltammetry, DPV) of BSA/QPRT/RGO/ITO electrode as a function of QA concentration [ranging from 6.5 μM to 65 mM] (b) Linearity between peak current of the bio-electrode measured by differential pulse voltammetry (DPV) and QA concentration has been shown on Log scale (c) Electrochemical current response studies (cyclic voltammetry, CV) of BSA/QPRT/RGO/ITO electrode as a function of time (days) and (d) Electrochemical current response studies (differential pulse voltammetry, DPV) of five different bio-electrodes BSA/QPRT/RGO/ITO fabricated via same set of procedure.

$$\Delta E_p(\mathrm{V})_{(\mathrm{RGO/ITO})} = [0.015\ \mathrm{V}(s/\mathrm{mV}) \times (\text{scan rate}(\mathrm{mV}/s))^{1/2}] + 0.11\ V,$$
$$R^2 = 0.999,\ \ SD = 1.31 \times 10^{-3}$$
$$\Delta E_p(\mathrm{V})_{(\mathrm{BSA/QPRT/RGO/ITO})} = [0.016\ \mathrm{V}(s/\mathrm{mV}) \times (\text{scanrate}(\mathrm{mV}/s))^{1/2}] + 0.13\ V, \quad (5)$$

$$R^2 = 0.998,\ \ SD = 1.78 \times 10^{-3} \quad (6)$$

where R is the correlation coefficient and SD is the standard deviation.

The diffusion coefficient (D) of bio-electrode BSA/QPRT/RGO/ITO was calculated using Randle Sevick equation (Kumar et al., 2016) (Eq. (7)) and found to be 0.31 $cm^2\ s^{-1}$.

$$I_p = (2.69 \times 10^5)\ n^{3/2} A\ D^{1/2} C\ \upsilon^{1/2} \quad (7)$$

where Ip is the peak current of immunoelectrode, n is the number of electrons (1) transferred, A is the active surface area of the immunoelectrode (0.25 cm^2), D is the diffusion coefficient, C is the concentration of redox species (5 mmol cm^{-2}) and υ is the scan rate (50 mV/s). Surface concentration (γ) of BSA/QPRT/RGO/ITO electrode was determined by using Laviron's theory (Sharma et al., 2012) given by

$$I_p = n^2 F^2 \gamma A \upsilon (4RT)^{-1} \quad (8)$$

where I_p represents the peak current of electrode, n is the number of electrons (1) transferred, F is the Faraday constant (96485 C mol^{-1}), γ is the surface concentration of the absorbed electro-active species, A is the surface area of the electrode, ν is the scan rate (V/s), R is the gas constant (8.314 J $mol^{-1}\ K^{-1}$) and T is room temperature (25 °C or 298 K). The Eq. (8) yields Υ to be 4.42×10^{-8} mol cm^{-2}.

4.4. Differential pulse voltammetry measurements

Differential pulse voltammetery (DPV) studies were carried out to measure the electrochemical response of the fabricated bio-electrodes (BSA/QPRT/RGO/ITO) as a function of QA concentration varying from 6.5 μM to 65 mM in PBS (pH 7.0, 0.9% NaCl) containing 5 mM $[Fe(CN)_6]^{3-/4-}$ [Fig. 5(a)]. It was observed that the magnitude of current increased with increase in concentration of QA which can be attributed to the formation of enzyme-ligand complex at the electrode surface. This process of complex formation leads to electron release at the electrode surface. QPRT; a member of the phosphoribosyl family of enzymes has been recognized to catalyze the formation of nicotinic acid mononuleotide from QA and substrate 5-phosphoribosyl-1-pyrophosphate (Bello and Grubmeyer, 2010). In this process, QA binds first to QPRT which may cause release of electron at the electrode surface. In the present work this process was monitored through differential pulse voltammetry measurements. Furthermore, a linear correlation was obtained in the wide concentration range of 6.5 μM to 65 mM (R^2 =0.993, SD =4.71×10^{-4}) and follow Eq. (9). Linearity between peak current of the bio-electrodes measured by differential pulse voltammetry (DPV) and QA concentration shown on log scale has been depicted in Fig. 5(b). The sensitivity of the electrode is found to be 7.86 mA $\mu M^{-1}\ cm^{-2}$.

$$I_p(\mathrm{mA}) = 7.86\ \mathrm{mA}\ \mu M^{-1} cm^{-2} \times \log[\text{concentration}\ (\mu M)] + 0.143\ \mathrm{mA},$$
$$R^2 = 0.993,\ \ SD = 4.71 \times 10^{-4} \quad (9)$$

Several studies on different sensing techniques and sensing characteristic of the proposed electrochemical bio-sensor BSA/QPRT/

Table 1
Sensing characteristics of the proposed electrochemical bio-sensor BSA/QPRT/RGO/ITO summarized along with some results reported in the literature.

Detection techniques of quinolinic acid (QA)	Detection range	Detection limit	Sensitivity	Stability (days)	References
Radio enzymatic assay for quinolinic acid	–	2.5 pmol	–	–	Kumar et al. 2015
Capillary electrophoresis-mass spectrometry	0.4–40 μM	–	–	–	Kumar et al. 2016
Liquid chromatography with fluorimetric detection	0.36–68.8 nmol ml^{-1}	–	–	–	Leipnitz et al. 2005
Fluorimetric detection of quinolinic acid by catalytic activity of horseradish peroxidase	0.1–5 nmol ml^{-1}	0.04 nmol ml^{-1}	–	–	Mawatari et al. 1995
Electrochemical bio-sensor	**6.5 μM–65 mM**	**6.5 μM**	**7.86 mA $\mu M^{-1} cm^{-2}$**	**30**	**Present work**

RGO/ITO discussed above have been compared and summarized in Table 1.

The stability of the BSA/QPRT/RGO/ITO electrode was determined by CV studies at a regular interval of 5 days up to 45 days [Fig. 5(c)] and stored at 4 °C until further use. It was observed that magnitude of the peak current exhibited 95% response upto 30 days and there after the peak current decreased and reached to 80% at the end of 45 days. It indicates that the stability of the fabricated BSA/QPRT/RGO/ITO bio-electrode is upto ~30 days. In order to ensure reproducibility, five different bio-electrodes of constant surface area were prepared under similar conditions and their electrochemical responses were investigated by DPV studies. These bio-electrodes exhibit good reproducibility. Mean value of the current was found equal to ~119 μA. Each measurement was repeated for three times for each electrode and error bar was included accordingly. The relative standard deviation (RSD) for each bio-electrode was less than ~5% which showed the reproducibility of the fabricated bio-electrodes is high [Fig. 5(d)]. DPV measurements have also been carried out for the detection of QA in the real sample (serum) as shown in Fig. S3.

5. Conclusions

Early detection of endogenous neurotoxin, quinolinic acid may be helpful to the patients suffering from many neurological disorders such as Alzheimer's, Huntington's and HIV associated dementia (HAD) as well as deficiency of vitamin B_6. In this work selective, stable and reproducible bio-electrodes have been fabricated to detect quinolinic acid. The proposed bio-sensor based on electrochemical sensing may provide potential platform for the sensitive and selective detection of QA which can be used for the early detection of the neurological disorders and other diseases in the real samples in future.

Conflict of interests

The authors declare no competing financial interest.

Acknowledgements

Ranjana Singh is grateful to UGC, New Delhi, Govt. of India for providing financial support in terms of BHU research fellowship. One of the authors (TKG) is grateful to UGC for providing the research grant under the UGC Dr. D. S. Kothari Post-Doctoral Fellowship Scheme [No. F. 4-2/2006 (BSR)/PH/13–14/0108]. RKS is grateful to AvH Foundation, Germany, DST and CSIR, New Delhi, Govt. of India for support to procure Micro-Raman setup. AS is thankful to DST India (Project Code: DST/TSG/PT2012/68 & DST PURSE SCHEME 5050) and CAS-UGC, (Grant No. [F.530/7/CAS-V/2015/(SAPI)]); Departmental Programme for providing financial assistance.

Appendix A. Supporting information

Supplementary data associated with this article can be found in the online version at doi:10.1016/j.bios.2016.11.053.

References

Bello, Z., Grubmeyer, C., 2010. Biochemistry 49, 1388–1395.
Birley, S., Collins, J.F., Perkins, M.N., Stone, T.W., 1982. Br. J. Pharmacol. 77, 7–12.
Brown, R.R., Yess, N., Price, J.M., Linkswiler, H., Sawan, P., Hankes, L.V., 1965. J. Nutr. 87, 419–422.
Chen, Y., Meininger, V., Guillemin, G.J., 2009. Cent. Nerv. Syst. Agents Med. Chem. 9, 32–39.
Chikkaveeraiah, B.V., Liu, H., Mani, V., Papadimitrakopoulos, F., Rusling, J.F., 2009. Electrochem. Commun. 11, 819–822.
Compton, O.C., Jain, B., Dikin, D.A., Abouimrane, A., Amine, K., Nguyen, S.T., 2011. ACS Nano 5, 4380–4391.
During, M.J., Freese, A., Heyes, M.P., Swartz, K.J., Markey, S.P., Roth, R.H., Martin, J.B., 1989. FEBS Lett. 247, 438–444.
Foster, A.C., Okuno, E., Brougher, D.S., Shwarcz, R., 1986. Anal. Biochem. 158, 98–103.
Guillemin, G.J., 2012. FEBS J. 279, 1356–1365.
Guillemin, G.J., Brew, B.J., 2002. Redox Rep. 7, 199–206.
Guillemin, G.J., Kerr, S.J., Brew, B.J., 2004. Neurotox. Res. 7, 103–123.
Heyes, M.P., Saito, K.J., Crowley, S., Davis, L.E., Demitrack, M., Der, A.M., Dilling, L.A., Elia, J., Kruesi, M.J.P., Lackner, A., Larsen, S.A., Lee, K., Leonard, H.L., Markey, S.P., Martin, A., Milstein, S., Mouradian, M.M., Pranzatelli, M.R., Quearry, B.J., Salazar, A., Smith, M., Strauss, S.E., Sunderland, T., Swedo, S.W., Tourtellotte, W.W., 1992. Brain 115, 1249–1273.
Huang, Y., Dong, Shi, X., Li, Y., Li, C.M., Chen, L.-J.P., 2010. Nanoscale 2, 1485–1488.
Han, M.Y., Oezyilmaz, B., Zhang, Y., Kim, P., 2007. Phys. Rev. Lett. 98, 206805–206809.
Huang, X., Yin, Z., Wu, S., Qi, X., He, Q., Zhang, Q., Yan, Q., Boey, F., Zhang, H., 2011. Small 7, 1876–1902.
Kumar, S., Kumar, S., Tiwari, S., Srivastava, S., Srivastava, M., Yadav, B.K., Kumar, S., Tran, T.T., Dewan, A.K., Mulchandani, A., Sharma, J.G., Maji, S., Malhotra, B.D., 2015. Adv. Sci. 2 (8), 1500048.
Kumar, S., J.G, Maji, S., Malhotra, B.D., 2016. Biosens. Bioelectron. 78, 497–504.
Leipnitz, G., Schumacher, C., Scussiato, K., Dalcin, K.B., Wannacher, C.M.D., Wayse, A.T.D., Dutra, C.S., Wagner, M., Latini, A., 2005. Int. J. Dev. Neurosci. 23, 695–701.
Mawatari, K.-I., Oshida, K., Iinuma, F., Watanabe, M., 1995. Anal. Chim. Acta 302, 179–183.
Marcano, D.C., Kosynkin, D.V., Berlin, J.M., Sinitsakii, A., Sun, Z., Slesarev, A., Alemany, L.B., Lu, W., Tour, J.M., 2010. ACS Nano 4, 4806–4814.
Odo, J., Inoguchi, M., Hirai, A., 2009. J. Health Sci. 55, 242–248.
Pumera, M., Ambrosi, A., Bonanni, A., Chng, E.L.K., Poh, H.L., 2010. Trac-Trend Anal. Chem. 29, 954–965.
Pumera, M., 2011. Mater. Today 14, 308–315.
Park, S.J., Kwon, O.S., Lee, S.H., Song, H.S., Park, T.H., Janng, J., 2012. Nano Lett. 12, 5082–5090.
Patterson, J.I., Brown, R.R., 1980. J. Chromatogr. 182, 425–429.
Schwarcz, R., Pellicciari, R., 2002. J. Pharmacol. Exp. Ther. 303, 1–10.
Schwarcz, R., Guidetti, P., Sathyasaikumar, K.V., Muchowski, P.J., 2010. Prog. Neurobiol. 90, 230–245.
Stone, T.W., Connick, J.H., 1985. Neuroscience 15, 597–617.
Shoemaker, J.D., Elliott, W.H., 1991. J. Chromatogr. 562, 125–138.
Srivastava, S., Solanki, P.R., Kaushik, A., Ali, M.A., Srivastav, A., Malhotra, B.D., 2011. Nanoscale 3, 2971–2977.
Schwierz, F., 2010. Nat. Nanotechnol. 5, 487–496.
Srivastava, S., Kumar, V., Ali, M.A., Solanki, P.R., Srivastava, A., Sumana, G., Saxena, P.S., Joshi, A.G., Malhotra, B.D., 2013. Nanoscale 5, 3043–3051.
Sarkar, P., Nicholson, P.S., 1996. J. Am. Ceram. Soc. 79, 1987–2002.
Srivastava, R.K., Srivastava, S., Narayanan, T.N., Mahlotra, B.D., Vajtai, R., Ajayan, P.M., Srivastava, A., 2012. ACS Nano 6, 168–175.
Sharma, A., Pandey, C.M., Sumana, G., Soni, U., Sapra, S., Srivastava, A., Chatterjee, T., Malhotra, B.D., 2012. Biosens. Bioelectron. 38 (1), 107–113.
Taguchi, H., Koyama, S., Shimabyashi, Y., Iwai, K., 1983. Anal. Biochem. 131, 194–197.
Wang, X., Davis, I., Liu, A., Miller, A., Shamsi, S.A., 2013. J. Chromatogr. A 1316, 147–153.
Zhang, Z., Chen, H., Xing, C., Guo, M., Xu, F., Wang, X., Gruber, H.J., Zhang, B., Tang, J., 2011. Nano Res. 4, 599–611.